Characterization of $MoSe_2(0001)$ and ion-sputtered $MoSe_2$ by XPS

WA'EL A. ABDALLAH, A. E. NELSON*
Department of Chemical and Materials Engineering, University of Alberta, Edmonton, Alberta, Canada, T6G 2G6
E-mail: alan.nelson@ualberta.ca

Molybdenum dichalcogenides (MoS_2, $MoSe_2$, $MoTe_2$) have attracted significant attention because of their primary importance as catalysts [1–3] and photovoltaic materials [4–6]. These materials have a hexagonal closed packed (hcp) structure that results from the stacking of weakly bonded X-Mo-X layers ($X = S$, Se, Te) and gives rise to highly anisotropic properties [7]. Of these, molybdenum disulfide (MoS_2) has been widely studied primarily due to its relevance as a hydrotreating catalyst to remove sulfur- and nitrogen-containing compounds from various oil fractions. The large basal plane (0001) of MoS_2 is relatively catalytically inactive, while the edge planes (S-edge, $\bar{1}010$; Mo-edge, $10\bar{1}0$) are generally accepted to be the active sites due to the presence of coordinatively unsaturated (*cus*) Mo (or promoter) sites. The $MoS_2(0001)$ surface has been shown to be catalytically inactive toward thiophene [8]; however, additional studies with ethanethiol have indicated slight reactivity suggesting the presence of *cus* sites on the freshly cleaved basal surface. Wiegenstein and Schulz [9] demonstrated the density of *cus* Mo sites can be increased using ion bombardment, thereby increasing the reactivity of methanethiol. Their XPS measurements of $MoS_2(0001)$ indicated that the Mo 3d peaks of a (0001) surface are consistent with Mo(IV), and no significant change in binding energy or intensity was observed after annealing to 573 K. However, following ion bombardment the Mo 3d peaks shifted to a higher binding energy consistent with a concentration of additional Mo oxidation states on the defective basal surface. Consequently, the $MoS_2(0001)$ surface can be made reactive using controlled ion bombardment to increase the density of *cus* sites.

In addition to the widespread application in the photovoltaic industry, $MoSe_2$ may also have the potential to be used as a nanostructured hydrotreating catalyst. For example, the mechanism of C—N bond cleavage in the hydrodenitrogenation (HDN) of aliphatic nitrogen-containing molecules has been suggested to be Hofmann-type elimination or nucleophilic substitution [10–14]. Both of these mechanisms require a pair of sites: an acid site to react with the nitrogen-molecule through the nitrogen atom, making the amine group ready to leave from the molecule; and a basic site to abstract the β-hydrogen in the elimination mechanism, or a nucleophile to attack the α-carbon in the nucleophilic substitution mechanism. It has been previously suggested that on a promoted (Ni) edge of MoS_2 ($10\bar{1}0$), the uncovered promoter atoms can accommodate the nitrogen-containing molecules as adsorption sites (Lewis acid sites) and the neighboring sulfur atoms can be the basic sites or the nucleophile [15]. Consequently, a favorable approach to increasing the reactivity is to increase the nucleophilic strength of the active site to promote the nucleophilic substitution mechanism. Comparing the nucleophilities of several compounds, $RSe^- > RS^- > R_2NH > NH_3 > H_2O$, selenium is the strongest nucleophile [10]. Therefore, promoted molybdenum diselenides are ideal materials for highly active and selective hydrodenitrogenation catalysts.

The objective of the present study is to present and interpret X-ray photoelectron spectroscopy (XPS) data of $MoSe_2(0001)$ and ion-sputtered $MoSe_2(0001)$ to deduce the surface chemistry of well-defined and defective surfaces. This characterization information will not only fill the current information gap, but also provide an indication whether $MoSe_2$ may be a potential candidate as a hydrotreating catalyst. Molybdenum selenide (0001) single crystals were obtained from Matek GmbH (Jülich, Germany) and used as received. X-ray photoelectron spectroscopic analysis was performed using a Kratos Axis 165 spectrometer with monochromatic Al Kα radiation. Survey (wide) spectra were collected from 0 to 1100 eV with a pass energy of 160 eV, step size of 0.33 eV, and a dwell time of 0.031 s (single scan), and high-resolution (narrow) spectra over the Mo 3d (224–238 eV), Se 3d (48–60 eV), and C 1s (279–289 eV) regions were acquired with a pass energy of 20 eV and a dwell time of 0.4 s (average of two scans). Argon ion sputtering was performed with a Kratos Mini Beam III operating at 3 kV with a system backpressure of 5.5×10^{-07} Torr for duration of 90 s. Peak deconvolutions of the high-resolution scans and atomic concentrations were calculated using the algorithm and sensitivity factors contained in the Kratos Vision2 software. Shirley-type background subtraction was performed and the high-resolution photoemission features were fitted with 70/30 Gaussian–Lorentzian peaks using a systematic approach.

Survey spectra of $MoSe_2(0001)$ and ion-sputtered $MoSe_2$ are shown in Figs 1 and 2, respectively, and the relative atomic concentrations of the elements are presented in Table I. The spectra show intense Mo 3p, Mo 3d, Se 3p and Se 3d photoemission features, in addition to Se LMM Auger peaks. Based on the integrated Mo 3d ($RSF = 3.321$) and Se 3d ($RSF = 0.853$) peak areas the Se/Mo ratio is 1.93, which is slightly less

---

*Author to whom all correspondence should be addressed.

0022–2461

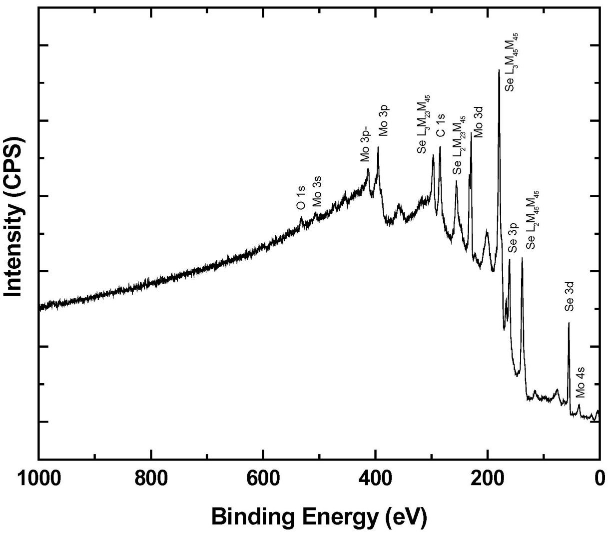

Figure 1 Survey (wide scan) X-ray photoelectron spectrum of $MoSe_2(0001)$, as received.

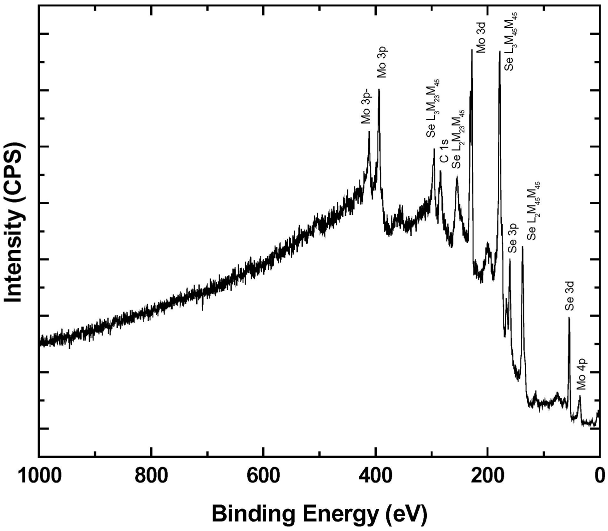

Figure 2 Survey (wide scan) X-ray photoelectron spectrum of ion-sputtered (90 s) of $MoSe_2$.

than the stoichiometric value of 2 suggesting a small quantity of surface defects (*cus* sites). The spectrum of $MoSe_2(0001)$ also indicates minor quantities of surface carbon (66.9 atom %) and oxygen (1.1 atom %). Selenium is preferentially removed from the surface after ion sputtering for 90 seconds giving rise to strong Mo photoemission features, as evidenced in Fig. 2. Additionally, the oxygen is completely removed and the carbon is slightly reduced (63.2 atom%) upon ion sputtering. The ratio of Se/Mo decreased to 1.07 indicating the stabilized stoichiometry is $MoSe_{1.07}$, which is in excellent agreement with a previous time resolved ion sputtering study of metal dichalcogenide compounds [16].

TABLE I Summary of spectral features

Element/transition	Binding energy (eV)[a]	FWHM (eV)	Conc. (atom %)[b]
	$MoSe_2(0001)$		
Mo 3d$_{5/2}$	229.3 (228.9)	0.49	10.9
Mo 3d$_{3/2}$	232.4 (232.0)	0.71	
Se 3d$_{5/2}$	54.9 (54.5)	0.49	21.1
Se 3d$_{3/2}$	55.7 (55.3)	0.56	
C 1*s*	285.4 (285.0)	1.27	66.9
O 1*s*	531.9 (531.5)	1.57	1.1
	Ion sputtered $MoSe_2$		
Mo 3d$_{5/2}$	227.9 (228.7)	0.52	17.8
Mo 3d$_{5/2'}$	228.5 (229.3)	0.60[c]	
Mo 3d$_{5/2''}$	229.0 (229.8)	0.60[c]	
Mo 3d$_{3/2}$	231.1 (231.9)	0.81	
Mo 3d$_{3/2'}$	231.9 (232.7)	0.60[c]	
Mo 3d$_{3/2''}$	232.3 (233.1)	0.60[c]	
Se 3d	54.7 (55.5)	1.43	19.0
C 1*s*	284.2 (285.0)	3.38	63.2

[a] The values in parentheses are corrected binding energies assuming the C 1s photoemission band corresponds to adventitious carbon at 285.0 eV.

[b] Atomic concentrations were quantified from the survey spectra.

[c] The FWHM for the peaks was constrained to 0.6 eV during peak fitting.

High-resolution analysis was performed over the Mo3d and Se 3d photoemission features to determine values for the relative binding energies, as summarized in Table I. The corrected binding energies presented in parentheses in Table I are calculated referencing the C 1s photoemission feature. High-resolution spectra of the C 1s features (not shown) indicate a chemical shift of +0.4 eV for $MoSe_2(0001)$ and −0.8 eV for ion-sputtered $MoSe_2$, assuming an adventitious C 1s photoemission band at 285.0 eV [17]. The observed charging effects are the result of electron loss from the surface by emission or electron gain by conduction or acquisition of slow or thermal electrons from the vacuum space. The high-resolution spectra of the Mo 3d features for $MoSe_2(0001)$ and ion-sputtered $MoSe_2$ are shown in Fig. 3a and b, respectively. The spectrum of

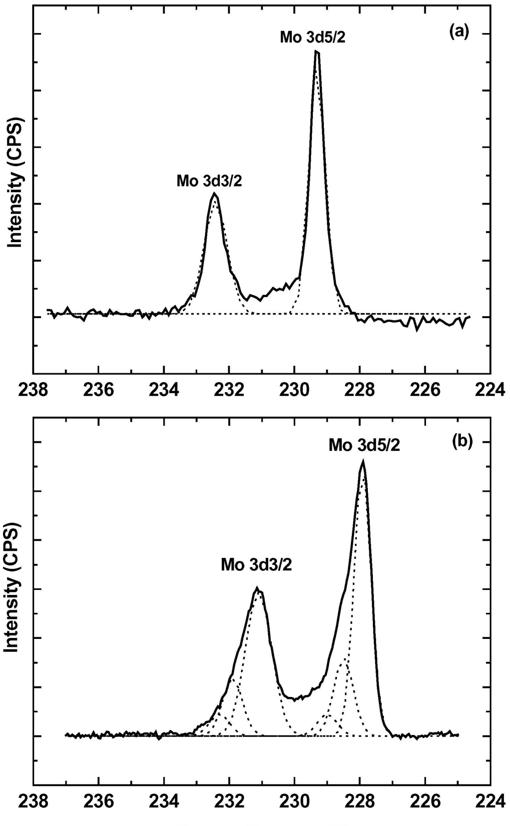

Figure 3 High-resolution (narrow scan) X-ray photoelectron spectra with peak deconvolutions of the Mo 3d binding energy region for: (a) $MoSe_2(0001)$ and (b) ion-sputtered $MoSe_2$. The binding energy scale is not corrected for observed charging effects.

$MoSe_2(0001)$ shows the Mo $3d_{5/2}$ and Mo $3d_{3/2}$ photoemission features with uncorrected binding energies of 229.3 and 232.4 eV, respectively, which is consistent with a Mo(IV) oxidation character after charge correcting [17, 18]. The region between the Mo $3d_{3/2}$ and Mo $3d_{5/2}$ also suggests the presence of the Se 3s photoemission band (ca. 230.5 eV) [19]; however no attempt was made to fit this feature. Ion sputtered $MoSe_2$ Mo 3d features are considerably broader indicating additional molybdenum surface oxidation states at higher binding energy. The individual Mo $3d_{5/2}$ and Mo $3d_{3/2}$ photoemission features were fit with three peaks, and the positions of these features are presented in Table I. The Mo $3d_{5/2}$ binding energy ranged from 227.9 to 229 eV and the Mo $3d_{3/2}$ binding energy ranged from 231.9 to 232.3 eV (uncorrected), indicating Mo(IV), Mo(V), and Mo(VI) surface oxidation states. This is in agreement with previous XPS observations of Mo surface chemistry of $MoS_2(0001)$ and ion bombarded MoS_2 [9]. The high-resolution spectra of Se 3d for $MoSe_2(0001)$ and ion-sputtered $MoSe_2$ are shown in Fig. 4a and b, respectively. The spectrum of $MoSe_2(0001)$ clearly indicates the Se $3d_{5/2}$ and Se $3d_{3/2}$ photoemission features with binding energies of 54.9 and 55.7 eV (uncorrected), respectively, Following ion bombardment, the Se 3d peak is significantly broadened over a range of 5 eV to include both the Se $3d_{5/2}$ and Se $3d_{3/2}$ photoemission features. Due to the apparent lack of distinguishable peaks, the peak fitting procedure produced subjective results which are not presented for additional discussion. It should be noted the Se 3d corrected binding energies are in excellent agreement with reference values [17].

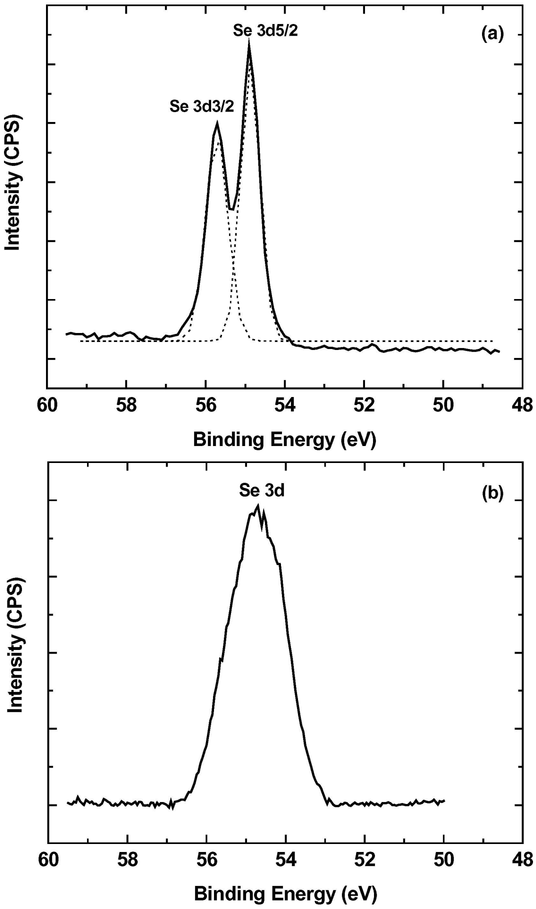

Figure 4 High-resolution (narrow scan) X-ray photoelectron spectra with peak deconvolutions of the Se 3d binding energy region for: (a) $MoSe_2(0001)$ and (b) ion-sputtered $MoSe_2$. The binding energy scale is not corrected for observed charging effects.

The XPS analysis in this report provides definitive information on the surface chemistry of $MoSe_2(0001)$, and the effects of ion sputtering on the preferential removal of selenium and the subsequent change in composition and surface chemistry. It is also apparent that $MoSe_2(0001)$ is susceptible to defect site formation through *ex situ* sample handling, or exposure to irradiation or UHV conditions. An acute knowledge of the relative surface chemistry and stability of $MoSe_2$ will support the development of nanocrystalline $MoSe_2$ for increased utilization in the photovoltaic industry and further the development of selenium-based heterogeneous catalysts.

Acknowledgments

The authors gratefully acknowledge financial support from Syncrude Canada Ltd. and the Natural Sciences and Engineering Research Council (NSERC) under the Industrial Research Chair for the Advanced Upgrading of Bitumen.

References

1. H. BOLIVAR, S. IZQUIERDO, R. TREMONT and C. R. CABRERA, *J. Appl. Electrochem.* **33** (2003) 1191.
2. T. J. BASTOW, *Solid State Nucl. Magn. Reson.* **12** (1998) 191.
3. T. KABE, A. ISHIHARA and W. QIAN, in "Hydrodesulfurization and Hydrodenitrogenation" (Wiley-VCH, Germany, 1999).
4. K. TOBIAS, T. YVONNE, T. MANUELA and T. HELMUT, *Solar Ener. Mat. Solar Cells.* **59** (1999) 309.
5. C. CLEMEN, X. I. SALDANA, P. MUNZ and E. BUCHER, *Phys. Stat. Sol. A: Appl. Res.* **49** (1978) 437.
6. T. WADA, N. KOHARA, S. NISHIWAKI and T. NEGAMI, *Thin Solid Films* **387** (2001) 118.
7. A. A. BALCHIN, in "Crystallography and Crystal Symmetry of Materials With Layered Structures," edited by F. Levey (Reidel, Dordrecht, 1976).
8. S. L. PETERSON and K. H. SCHULZ, *Langmuir* **12** (1996) 941.
9. C. G. WIEGENSTEIN and K. H. SCHULZ, *J. Phys. Chem.* B **103** (1999) 6913.
10. R. M. LAINE, *Catal. Rev. –Sci. Eng.* **25** (1983) 459.
11. N. NELSON and R. B. LEVY, *J. Catal.* **58** (1979) 485.
12. M. ZDRAZIL, *ibid.* **141** (1993) 316.
13. S. RAJAGOPAL and R. MIRANDA, *ibid.* **141** (1993) 318.
14. Y. ZHAO, P. KULULA and R. PRINS, *ibid.* **221** (2004) 441.
15. M. SUN, A. E. NELSON and J. ADJAYE, *ibid.* **226** (2004).
16. J. C. BERENDE, *Appl. Surf. Sci.* **171** (2001) 15.
17. J. F. MOULDER, W. F. STICKLE, P. E. SOBOL and K. D. BOMBEN, in "Handbook of X-ray Photoelectron Spectroscopy" (Physical Electronics, Inc., Eden Prairie, Minnesota, 1995).
18. S. O. GRIM and L. J. MATIENZO, *Inorg. Chem.* **14** (1975) 1014.
19. C. CALARESO, V. GRASSO and L. SILIPIGNI, *Appl. Surf. Sci.* **171** (2001) 306.

Received 1 July
and accepted 31 August 2004